

Received March 9, 2017, accepted April 4, 2017, date of publication April 14, 2017, date of current version May 17, 2017.

Digital Object Identifier 10.1109/ACCESS.2017.2694143

The Design of Directional Coupler for ECRH System

DAJUN WU^{1,2}, FUKUN LIU¹, XIAOJIE WANG¹, HANDONG XU¹, LIYUAN ZHANG¹, WEIYE XU¹, YUNYING TANG¹, AND JIAN WANG¹

¹Institute of Plasma Physics, Chinese Academy of Sciences, Hefei 230031, China

²University of Science and Technology of China, Hefei 230026, China

Corresponding author: Dajun Wu (djwu@ipp.ac.cn)

This work was supported by the National Magnetic Confinement Fusion Science Program of China under Grant 2011GB102000 and Grant 2015GB103000.

ABSTRACT A study of coupling characteristic between circular corrugated waveguide and rectangular smooth waveguide has been presented in this paper, which aims to develop a directional coupler integrated into a miter bend for an electron cyclotron resonance heating system on EAST. The performances of the several aperture array distributions are analyzed based on the aperture diffraction theory in detail. The broadband, good in-band coupling flatness, and excellent directivity are achieved by using the proposed novel aperture array on the mirror surface. For verification purpose, a prototype of the directional coupler has been designed and fabricated.

INDEX TERMS Directional coupler, ECRH, aperture coupling, miter bend.

I. INTRODUCTION

Directional couplers are the key components in microwave and millimeter wave applications for power measurement. For ECRH system on Tokamak or stellarator, in order to monitor the millimeter wave power in real time, directional couplers integrated in miter bend are required for corrugated waveguide transmission line [1], [2]. It mainly consists of hole array on mirror surface and fundamental rectangular waveguide below the mirror surface. The electromagnetic (EM) waves coupled to the auxiliary waveguide via holes cancel in one direction while add in the other direction. A directional coupler with double apertures has been developed [3]. Its coupling factor is about -70 dB, and directivity is greater than 17 dB from 138 GHz to 142 GHz. To obtain high directivity and wide bandwidth, multi-aperture coupling method has been used [4]–[6].

The dimension and location of aperture dominate coupling performance for any coupler. In this work, we focus on studying the relationship between coupler performance and multi-aperture parameter by using the aperture diffraction theory and phase superposition principle. Firstly, the geometry of coupler and the coupling characteristic for a single aperture are described. Then several representative aperture array distributions are adopted to optimize the coupler. At last, a prototype of coupler integrated in miter bend with optimal aperture array parameter has been manufactured for verification.

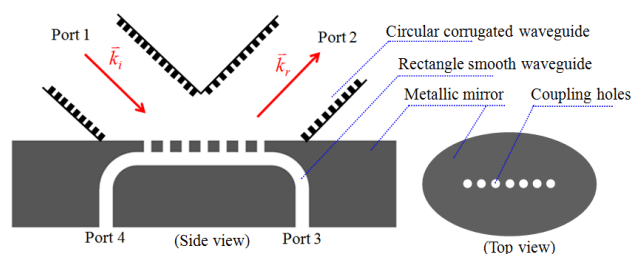


FIGURE 1. The structure of the directional coupler.

II. PRINCIPLE OF THE DIRECTIONAL COUPLER

Fig. 1 shows the side view and top view (only mirror) of a typical corrugated waveguide directional coupler structure. A linear array of drilling holes along the mirror center couples incident power from main line to mini rectangular waveguide embedded in mirror body.

The coupling coefficient (C), directivity (D) of directional coupler are defined as follows:

$$C = 10 \log_{10} \frac{P_3}{P_1} \quad (1)$$

$$D = 10 \log_{10} \frac{P_3}{P_4} \quad (2)$$

Where P_1 is the incident power, P_3 is the coupled power, P_4 is the power out of isolation port. Either broad or narrow

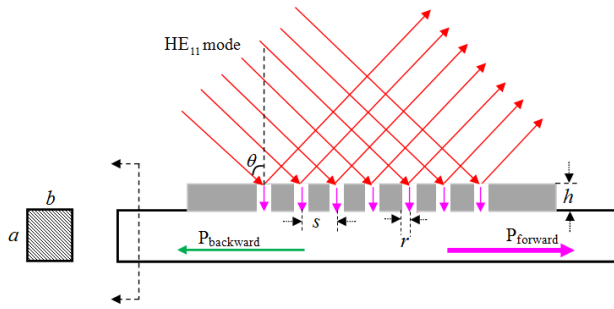


FIGURE 2. The schematic diagram of coupler.

side of rectangular waveguide can be used for holes drilling. The schematic diagram of this coupler (narrow side case only) is shown in Fig. 2.

According to the aperture diffraction theory [7], when the EM wave is coupled to an auxiliary waveguide from primary one via an aperture, the corresponding coupling strength is expressed as:

$$A^{\pm} = -\frac{j\omega}{2}(\epsilon_0 \cdot p \cdot E_{2n}^{\pm} \cdot E_{1n}^+ + \mu_0 \cdot p^* \cdot H_{2t}^{\pm} \cdot H_{1t}^+) \quad (3)$$

Where A^{\pm} are coupling strength of the forward wave (plus sign) and backward wave (minus sign) in the auxiliary waveguide, p and p^* are electric polarizability and magnetic polarizability, respectively. E_{1n}^+ and E_{2n}^{\pm} refer to normal electric field amplitudes in primary waveguide and auxiliary waveguide, H_{1t}^+ and H_{2t}^{\pm} refer to corresponding tangential magnetic ones, ω is the angular frequency, θ is the angle of incidence. The transmitting powers of both lines need be normalized to the same level for computation. According to Eq. (3), coupling feature between the primary and the auxiliary waveguide can be divided into electric coupling, magnetic coupling and electromagnetic coupling depended on which component is used.

III. DESIGN OF DIRECTIONAL COUPLER

A. SELECTION OF E PLANE OR H PLANE MITER BEND

In ECRH system, the polarization of the beam from the gyrotron entering into the MOU is usually horizontal, and the coupler (also named power monitor bend) will be installed before polarizer in ECRH transmission line. Thus, the wave arriving at the coupler mirror has a linear polarization state. According to different assembling positions, the miter bend is divided into E plane bend (electric field in the plane of incidence) and H plane bend (electric field in the perpendicular plane), respectively. Two different auxiliary waveguide structures sketched in Fig. 3 must be considered to match these orthogonal polarizations.

Combining the Eq. (3) and the coordinate system of Fig. 3, we can find that magnetic and electric coupling will happen simultaneously for E plane, but for H plane only magnetic coupling exists. Coupling intensity can be described or calculated using these equations:

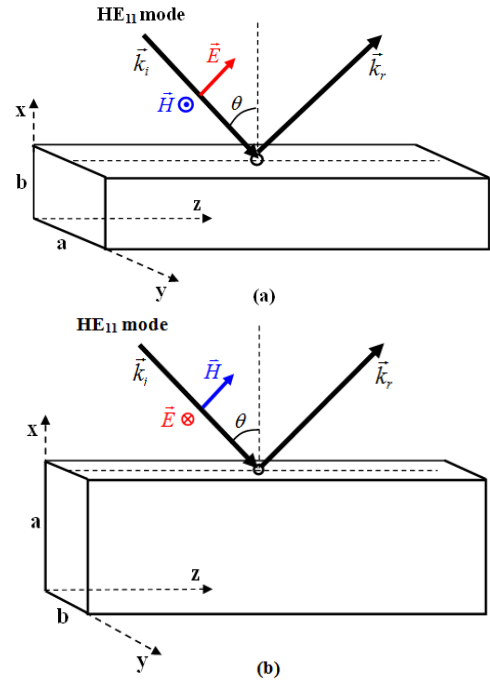


FIGURE 3. Two coupling waveguide structures for miter bend (a) E plane (b) H plane.

For E plane:

$$A_k^{\pm} = -\frac{j\omega}{2}(\epsilon_0 \cdot p \cdot E_{2x}^{\pm} \cdot E_{1x}^+ + \mu_0 \cdot p^* \cdot H_{2y}^{\pm} \cdot H_{1y}^+) \quad (4)$$

For H plane:

$$A_k^{\pm} = -\frac{j\omega}{2}(\mu_0 \cdot p^* \cdot H_{2z}^{\pm} \cdot H_{1z}^+) \quad (5)$$

For a plane miter bend, the theoretical ohmic loss on metallic mirror surface can be calculated as [8]:

$$P_{L1} = P_{in} \cdot \frac{4}{\cos \theta} \sqrt{\frac{\pi \epsilon_0 f}{\sigma}} \quad (\text{E plane reflection}) \quad (6)$$

$$P_{L2} = P_{in} \cdot 4 \cos \theta \sqrt{\frac{\pi \epsilon_0 f}{\sigma}} \quad (\text{H plane reflection}) \quad (7)$$

Where, P_{in} is the incident power density, σ is the conductivity of the mirror surface. For 45 deg incidence angle θ , P_{L1} is double of P_{L2} theoretically. Meanwhile, drilling holes on surface will unavoidably result in additional loss. In order to increase the power handling ability in the case of up to 1 MW continuous wave (CW) operation, we will choose H plane miter bend as coupler body in this work.

B. ANALYSIS FOR SINGLE HOLE

To make all the coupling EM power from different holes add at the end of rectangular waveguide without phase difference, the phase constant of HE_{11} mode in primary waveguide and TE_{10} mode in auxiliary one should satisfy the relation below:

$$\beta_{HE_{11}} \cdot \sin \theta = \beta_{TE_{10}} \quad (8)$$

Broad wall value $a = 1.52$ mm can be obtained by solving Eq. (8) with incidence angle $\theta = 45$ deg. The corresponding narrow wall value b is chosen as 0.83 mm to form a closed rectangular waveguide, this dimension is a slightly larger than standard waveguide for more space to drill. Taking into account shaping feasibility, round hole is a good choice as coupling aperture for this work. With regard to round hole, p and p^* in Eq. (3) have the expressions below:

$$p = \frac{2}{3}r^3, p^* = \frac{4}{3}r^3 \quad (9)$$

Where r is the radius of the hole. The normalized magnetic field amplitudes shown in Eq. (5) of circular corrugated waveguide and rectangular smooth waveguide are as follows:

$$H_{1z} = \frac{\sqrt{Z_{11}}}{\sqrt{\pi A} |J_1(X_{11})|} J_0\left(\frac{X_{11} \cdot R}{A}\right) \cos \theta \quad (10)$$

$$H_{2z} = -j \frac{\sqrt{Z_{10}}}{Z_0} \frac{\pi}{ak_0} \sqrt{\frac{2}{ab}} \quad (11)$$

Where k_0 and Z_0 are the phase constant and wave impedance in free space. Z_{11} and Z_{10} refer to the wave impedance of HE_{11} mode and TE_{01} mode, J_0 and J_1 are the zero and first order Bessel function. X_{11} is the balanced HE_{11} eigenvalue 2.405 and R is the distance from central axis of corrugated waveguide with radius $A = 31.75$ mm.

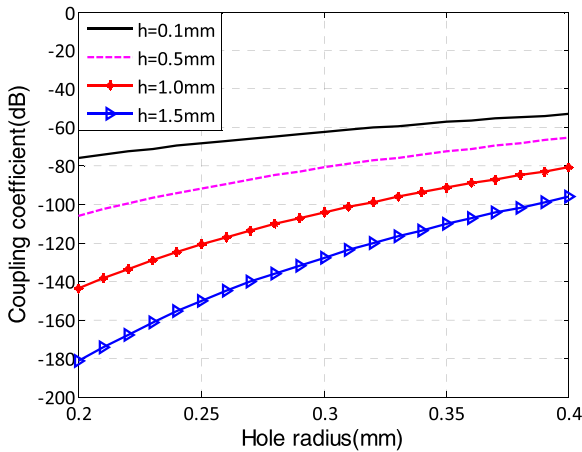


FIGURE 4. Coupling coefficient varying with the depth of single hole.

The coupling round hole acts as a short section of smooth circular waveguide for coupled power. The maximum hole diameter drilled on narrow wall is less than wall width 0.83 mm which will cause the lowest TE_{11} mode to cut off below 212 GHz. For the convenience of calculation, we assume a TE_{11} waveguide mode in the hole with the depth of h , and just take the $\alpha \cdot h$ as additional attenuation factor, α is attenuation constant of TE_{11} mode. Fig. 4 shows the calculated coupling coefficient varying with the depth for a single hole located at the center of mirror with the frequency 140 GHz. It is obvious that more than one hole should be drilled to achieve coupling factor less than -60 dB.

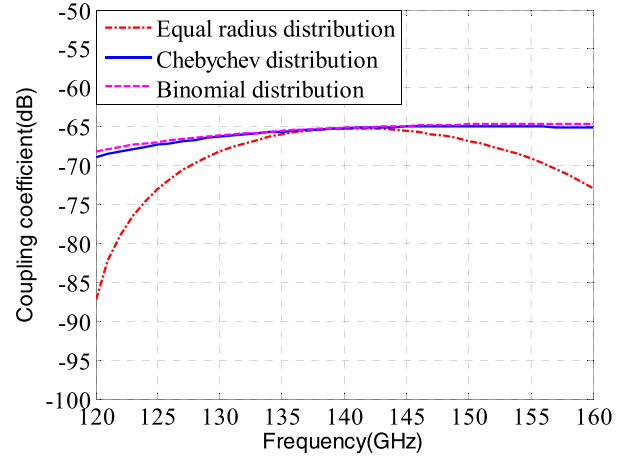


FIGURE 5. The computed coupling coefficient of 17 holes.

C. ANALYSIS FOR MULTI-HOLE

In order to eliminate high order diffraction modes, the hole interval is limited less than half wavelength, so the value of s is set as 1mm. From the Eq. (10) and Fig. 3, the amplitude of H_{1z} associated with the k -th coupling hole is given by:

$$H_{1z}(k) = \frac{\sqrt{Z_{11}}}{\sqrt{\pi A} |J_1(X_{11})|} J_0\left(\frac{X_{11} \cdot R(k)}{A}\right) \cos \theta \quad (12)$$

The amplitude H_{2z} keeps constant along the hole array. Adding the attenuating effect from each hole depth, the coupling strength contributed by k -th hole is deduced as:

$$A^\pm(k) = -\frac{j\omega}{2} [\mu_0 \cdot p^*(k) \cdot H_{2z}^\pm \cdot H_{1z}^\pm(k)] \cdot e^{-j\alpha(k)h} \quad (13)$$

In consideration of the phase delay due to wave propagation in the main and coupled waveguides, the contributions of all coupling holes to the forward and backward wave at two ends of the auxiliary waveguide are expressed as:

$$A_{\text{forward}} = \sum_{k=1}^N A^+(k) \cdot \exp[-i \cdot (k-1) \cdot \sin \theta \cdot s \cdot \beta_{HE11} - i \cdot (N-k) \cdot s \cdot \beta_{TE10}] \quad (14)$$

$$A_{\text{backward}} = \sum_{k=1}^N A^-(k) \cdot \exp[-i \cdot (k-1) \cdot \sin \theta \cdot s \cdot \beta_{HE11} - i \cdot (k-1) \cdot s \cdot \beta_{TE10}] \quad (15)$$

As described in previous section, each hole will add an exponential attenuation factor for coupled power. So more and bigger holes should be employed to compensate this loss for deeper hole. The hole array appeared on mirror surface will weak the reflection property and increase relevant loss. From this view, we need decrease the depth of the hole in design. On the other hand, decreasing the depth of hole will increase shaping difficulty and weaken mechanical strength. Meanwhile more holes mean the higher directivity for coupler. Thus, we need balance requirements mentioned above in actual design. In this paper we will choose 0.8 mm as the hole depth.

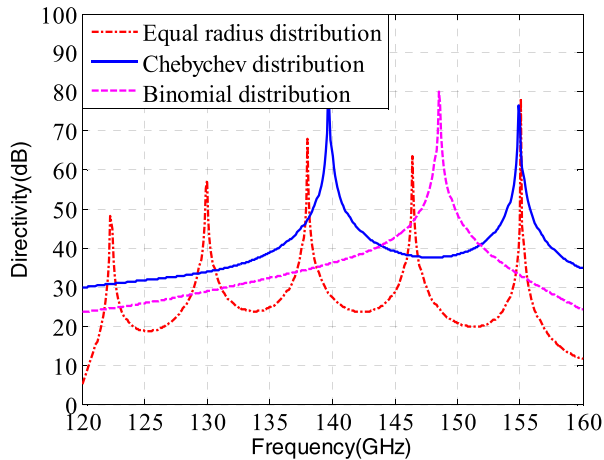


FIGURE 6. The computed directivity of 17 holes.

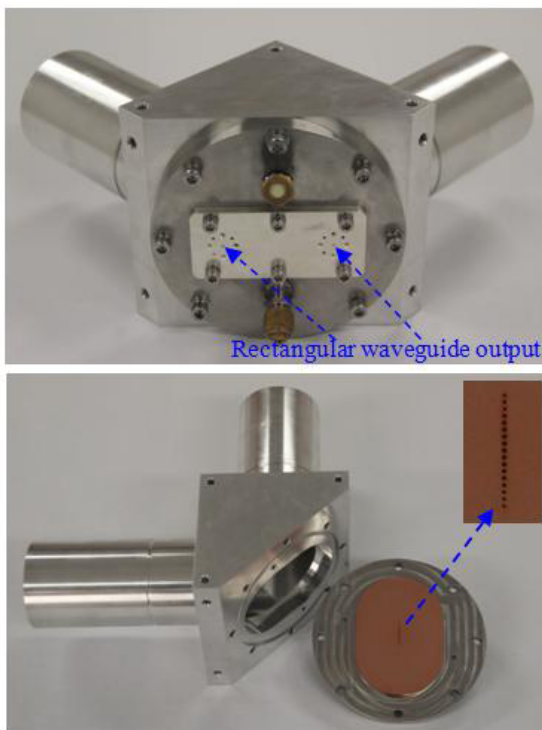


FIGURE 7. The photographs of fabricated directional coupler.

The arrangement of each aperture size will directly decide coupler performance after the aperture shape and the interval finalized. In present design, the general principle is to seek the optimal coupling strength distribution by adjusting each hole radius. Chebychev polynomial is widely used in microwave device design, such as filter, impedance transformer and directional coupler [9]. Coupling strength distribution by hole array obeying Chebychev rule can yield higher directivity and wider bandwidth than other cases. Thus, after repeating the calculations, the total 17 holes whose radius range from 0.20 to 0.37 mm are finally chosen to approximate a special Chebychev coupling distribution. Two other cases of binomial and equal radius coupling distributions with same hole

number are also calculated for comparison. The results are shown in Fig. 5 and Fig. 6.

From the results above, the desired -65 dB coupling coefficient has been realized at the central frequency 140 GHz by each distribution, but the flatness of both Chebychev and binomial are quite better than the equal radius case. The directivity of Chebychev is in excess of 60 dB at the central frequency. It is still greater than 30 dB from 120 to 160 GHz, the mean value is about 5 dB higher than binomial case.

D. MANUFACTURE OF PROTOTYPE

A prototype of this power monitor with Chebychev distribution has been fabricated, as shown in Fig. 7. The inner diameter of input or output normal circular corrugated waveguide is 63.5 mm. The width, period and depth of corrugation are chosen as 0.45 mm, 0.65 mm and 0.54 mm, respectively. Aluminum alloy is used as material for light weight. The holes are drilled on the copper mirror along the central line. The buried rectangle waveguide is extended to the back of mirror, and two waveguide ends with special flange type are reserved for components such as detector, attenuator and matched load assembly. In addition, the mirror body integrates necessary cooling water channels for high power CW operation.

IV. CONCLUSIONS

A -65dB directional coupler integrated in miter bend is designed in this paper. The coupling characteristic and the influence of aperture parameter to coupler performance have been investigated in detail. The novel proposed aperture array distribution improves the directivity considerably. A coupler prototype with cooling water channels has been successfully fabricated and the test work is under preparation.

ACKNOWLEDGMENTS

We would like to thank Prof. S. Kubo (National Institute for Fusion Science, Toki) and Prof. W. Kasperek (University of Stuttgart, Stuttgart) for fruitful discussion and kind assistance.

REFERENCES

- [1] F. Leuterer *et al.*, "Experience with the ECRH system of ASDEX-Upgrade," *Fusion Eng. Design*, vol. 53, pp. 486–487, Jan. 2001.
- [2] W. Kasperek *et al.*, "Status of the 140 GHz, 10 MW CW transmission system for ECRH on the stellarator W7-X," *Fusion Eng. Design*, vol. 74, pp. 243–248, Nov. 2005.
- [3] L. Qin, Q. Zhao, and S. Z. Liu, "Design of millimeter-wave high-power power monitoring miter bend based on aperture-coupling," *Plasma Sci. Technol.*, vol. 16, no. 7, pp. 712–713, Jul. 2014.
- [4] T. Notake *et al.*, "Real time polarization monitor developed for high power electron cyclotron resonance heating and current drive experiments in large helical device," *Rev. Sci. Instrum.*, vol. 76, no. 2, p. 023504, 2005.
- [5] W. Kasperek, H. Idei, S. Kubo, and T. Notake, "Beam waveguide reflector with integrated direction-finding antenna for *in-situ* alignment," *Int. J. Infr. Millim. Waves*, vol. 24, no. 4, pp. 458–459, Apr. 2003.
- [6] J. Ruiz *et al.*, "Numerical and experimental investigation of a 5-port miter-bend directional coupler for mode analysis in corrugated waveguides," *J. Infr. Millim. Terahertz Waves*, vol. 33, no. 5, pp. 491–504, May 2012.

- [7] H. J. Huang, *Microwave Principle*. Beijing, China: Science Press, 1965, pp. 223–231.
- [8] M. Lennholm *et al.*, “The ECRH/ECCD system on Tore Supra, a major step towards continuous operation,” *Nucl. Fusion*, vol. 43, no. 11, pp. 1460–1461, Nov. 2003.
- [9] J. H. Gu, *Microwave Technology*. Beijing, China: Science Press, 2004, pp. 290–296.



DAJUN WU received the B.S. degree in electrical and information engineering from Anhui Polytechnic University, Anhui, China, in 2005. He is currently pursuing the Ph.D. degree in nuclear science and engineering with the University of Science and Technology of China, Hefei, China. He is currently with the Institute of Plasma Physics, Chinese Academy of Sciences, Hefei, China.

His research interests include high-power microwave heating technology for plasma and electromagnetic field analysis.

FUKUN LIU is currently a Professor with the Institute of Plasma Physics, Chinese Academy of Sciences, Hefei, China. His research interests include microwave technology and experimental plasma physics.

XIAOJIE WANG is currently an Associate Researcher with the Institute of Plasma Physics, Chinese Academy of Sciences, Hefei, China. Her research interests include microwave technology and experimental plasma physics.

HANDONG XU is currently a Senior Engineer with the Institute of Plasma Physics, Chinese Academy of Sciences, Hefei, China. His research interests include high-power microwave heating technology and experimental plasma physics.

LIYUAN ZHANG is currently with the Institute of Plasma Physics, Chinese Academy of Sciences, Hefei, China. His research interests include mechanical design.

WEIYE XU is currently with the Institute of Plasma Physics, Chinese Academy of Sciences, Hefei, China. His research interests include high-power microwave heating and electronic technology.

YUNYING TANG is currently with the Institute of Plasma Physics, Chinese Academy of Sciences, Hefei, China. Her research interests include electromagnetic analysis.

JIAN WANG is currently with the Institute of Plasma Physics, Chinese Academy of Sciences, Hefei, China. His research interests include water cooling technology.

• • •